

# Non-Linearity Characterization of Submicron Type-I InP/InGaAs/InP and Type-I/II AlInP/GaAsSb/InP DHBTs

Huiming Xu, Eric Iverson, K.Y. (Donald) Cheng, Mark Stuenkel and Milton Feng

Department of Electrical and Computer Engineering, University of Illinois at Urbana-Champaign,  
208 North Wright Street, Urbana, IL61801 Tel./Fax: (217)244-3662, Email: xu24@illinois.edu

**Keywords: Indium Phosphide, Heterojunction Bipolar Transistor, Nonlinearity**

## Abstract

**A novel Type-I/II DHBT with AlInP emitter and GaAsSb base layers has been developed which demonstrates high gain, balanced  $f_T/f_{MAX} > 400$  GHz and  $BV_{CEO} > 4$  V. Due to its favorable band alignment, Type-I/II DHBT shows superior DC and RF linearity performance compared with foundry-provided Type-I DHBTs.**

## INTRODUCTION

InP based single heterojunction bipolar transistors (SHBTs) have demonstrated high-speed transistor operation with current gain cutoff frequency ( $f_T$ ) exceeding 850 GHz via the use of a graded bandgap InGaAs base and collector [1]. However, InP SHBTs suffer from low  $BV_{CEO} = 1.65$  V and thus are useful for low voltage and low power operation. Mixed signal circuits require transistors exhibiting high breakdown voltage, thermal conductivity and linearity to improve dynamic range. Foundries provide two types of InP based DHBTs to address the requirement of higher breakdown voltage, namely, Type-I InP/InGaAs/InP DHBT and Type-II GaAsSb/InP DHBT. Recently, a novel Type-I/II DHBT with AlInP emitter and GaAsSb base layers has been developed which demonstrates high gain, balanced  $f_T/f_{MAX} > 400$  GHz and  $BV_{CEO} > 4$  V [2]. In this work, we have benchmarked the DC and RF linearity performance of submicron Type-I/II DHBT made at UIUC against similar-geometry Type-I DHBTs obtained from two commercial foundries.

## EPITAXIAL LAYER STRUCTURE AND PROCESS

Type-I/II InP DHBT epitaxial wafers were grown by solid source MBE at UIUC. The structure consists of a 200 nm InGaAs subcollector, a 100 nm InP collector lightly doped to  $n = 5 \times 10^{16} \text{ cm}^{-3}$  to achieve a high breakdown voltage, a 17 nm carbon-doped GaAsSb base, an AlInP emitter graded to InP, and a 40 nm compositionally graded emitter cap ( $\text{In}_{0.53}\text{Ga}_{0.47}\text{As}$  to InAs). Devices with emitter widths ranging from 0.3-0.5  $\mu\text{m}$  were fabricated using electron beam lithography, wet-etch and passivated with BCB at UIUC microelectronics facility [2]. A scanning electron micrograph of a  $0.35 \times 3 \mu\text{m}^2$  device cross-section view after planarization and RF pad metallization is shown in Fig. 1(a). The top view of the device before passivation is shown in Fig. 1(b). The

emitter contact layer is connected to the coplanar waveguide. The foundry-provided Type-I InP/InGaAs/InP DHBT uses an InGaAs collector super-lattice transition layer to alleviate the current blocking effect [3]. The detailed layer structures of a Type-I and Type-I/II DHBTs studied in this work have already been shown in previous studies [4].

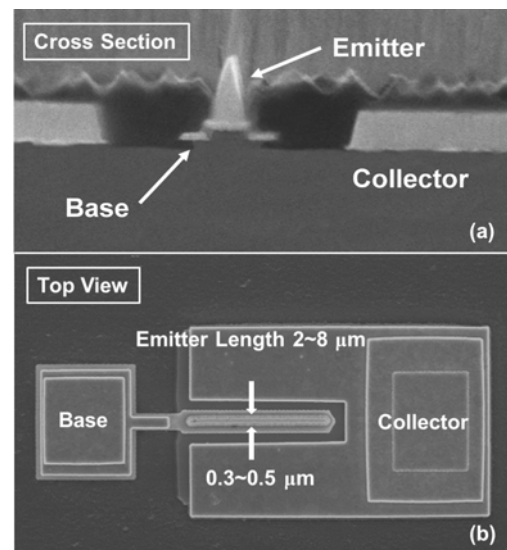


Figure. 1. Scanning electron microscopy of a fabricated DHBT: (a) Cross-section view of the device after coplanar RF pad metallization. (b) top view of the device before passivation. Emitter length ranges from 2 to 8  $\mu\text{m}$ , and emitter width varies from 0.3 to 0.5  $\mu\text{m}$ .

## DC CHARACTERISTICS

The collector I-V family curves of two foundry-provided (Foundries A&B) Type-I DHBTs are characterized and compared to UIUC Type-I/II DHBTs (Fig. 2 (a) and (b)). The Type-I/II DHBT demonstrates a much lower knee voltage (less than 0.62V at  $J_C = 10 \text{ mA}/\mu\text{m}^2$ ) than the Type-I device with the same bias current (greater than 1.0V at  $J_C = 10 \text{ mA}/\mu\text{m}^2$ ). Smaller knee voltage progression shown in the Type-I/II DHBT indicates its suitability for linear amplification at lower bias voltage. Our measurements indicate that the InGaAs collector super-lattice transition layer in Type-I DHBT is only effective at low collector

current density levels. At high collector current densities, electrons still experience an energy barrier at the InGaAs/InP hetero-junction, resulting in current blocking. For the Type-I/II DHBT, due to its favorable base-collector band alignment, there is no current blocking issue. The negative slope of family curves at high  $V_{CE}$  is due to the temperature rise in the device when  $V_{CE}$  is increased.

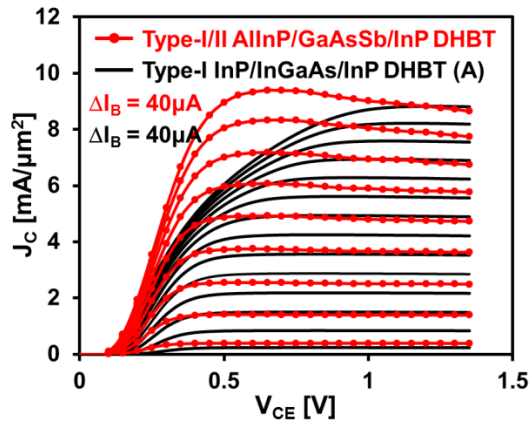


Figure. 2(a): Collector I-V of UIUC Type-I/II DHBT (red lines with dots) and Foundry-A Type-I DHBT (black lines). The Foundry-A device exhibits higher knee voltage and considerable gain compression at high collector current densities.

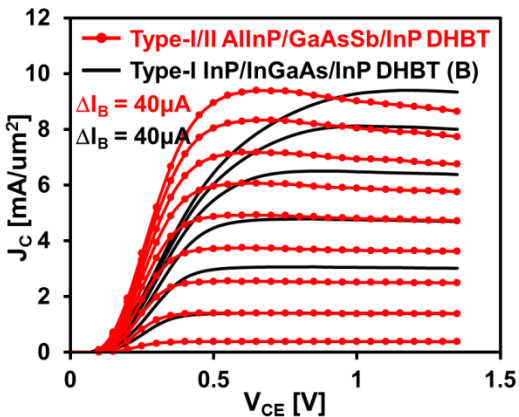


Figure. 2(b): Collector I-V of UIUC Type-I/II DHBT (red lines with dots) and Foundry-B Type-I DHBT (black lines). The Foundry-B device exhibits higher knee voltage and considerable gain compression at high collector current densities.

Fig. 3 illustrates the current gain compression shown in the above two family curves: the UIUC Type-I/II device shows little compression, but both foundry Type-I devices suffer  $>35\%$   $\beta$  reduction at high collector current densities and fixed  $V_{CE} = 1V$ . This is due to current blocking resulting from conduction band alignment at the base-collector junction.

Both current gain compression and higher knee voltage would lead to the nonlinear operation of the transistor.

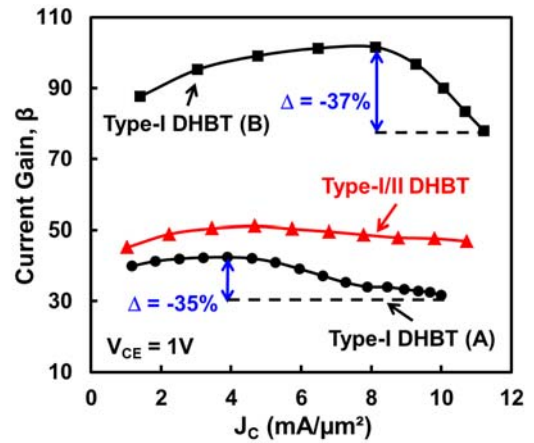


Figure. 3: Both Type-I InP DHBTs exhibit  $\beta$  compression with  $>35\%$  drop in current gain at high current density. UIUC Type-I/II InP DHBT shows minimal  $\beta$  variation. Current gain compression can lead to nonlinearity in device operation.

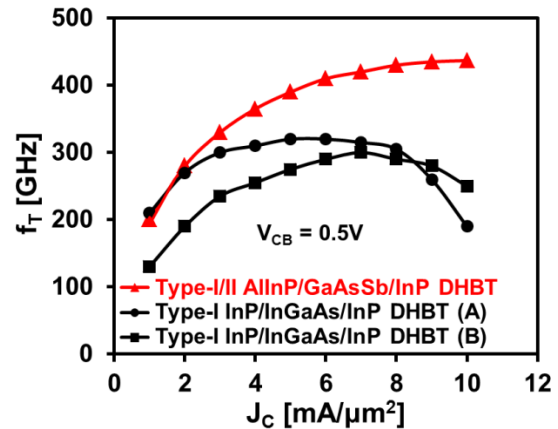


Figure. 4: Both Type-I devices show  $f_T$  fall-off behavior at high collector current density levels. Type-I/II DHBT  $f_T$  increases monotonically with collector current density.

#### RF CHARACTERISTICS

To further investigate the influence of band alignment on device microwave performance, S-parameters and two tone inter-modulation distortion were measured and compared for the two types of DHBTs. S-parameters were measured from 0.5GHz to 50GHz by an Agilent 8364A Power Network Analyzer, using off-wafer SOLT calibration and on-wafer short-open de-embedding method. Current gain cut off frequency  $f_T$  was extracted from current gain ( $H_{21}$ ) vs frequency curve using single pole fitting method. Fig. 4 shows the extracted  $f_T$  vs  $J_C$  for Type-I/II and Type-I DHBTs. For both Type-I DHBTs,  $f_T$  falls off at high current densities, due to carrier blocking at B/C junction, base push-out and

charge accumulation effects. The  $f_T$  fall off shows that the InGaAs collector super-lattice transition layer in the collector of Type-I DHBTs is insufficient to resolve the current-blocking problem and could cause additional base push-out and charge accumulation problem resulting in performance degradation of the transistor [4].

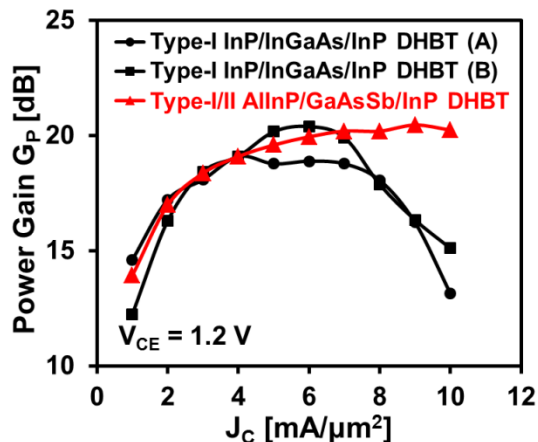


Figure 5. (Color online) Type-I/II DHBT Power Gain  $G_p$  increases monotonically with collector current density. Type-I DHBT power gain increases with collector current density at first but fall off at high collector current density levels ( $J_c > 6 \text{ mA}/\mu\text{m}^2$ ).

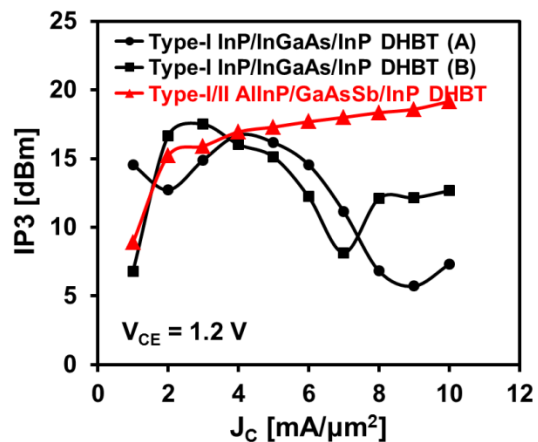


Figure 6. (Color online) Type-I/II DHBT  $IP_3$  increases monotonically with collector current density. Type-I DHBT  $IP_3$  increases with collector current density at first but fall off at high collector current density levels ( $J_c > 4 \text{ mA}/\mu\text{m}^2$ ).

#### NONLINEARITY CHARACTERISTICS

Previous studies on silicon BJTs by Poon [5] and GaAs SHBTs by Asbeck [6] have demonstrated a correlation between the variance of  $f_T$  vs  $J_c$  curve and the third-order intercept point  $IP_3$ , which is an important measure of transistor nonlinearity. It was shown that transistor with smaller variance on  $f_T$  vs  $J_c$  curve will have higher  $IP_3$ , while

transistor with larger variance of on  $f_T$  vs  $J_c$  curve will have lower  $IP_3$ , thus worse linearity performance. However, it was not clear the same correlation exists in InP DHBTs, as the physical origins of nonlinearity in InP DHBTs would be different from those of silicon BJTs and GaAs SHBTs because of the hetero-interface in the base-collector junction. To characterize transistor nonlinearity, two-tone intermodulation distortion was measured using two microwave sources of HP 83621A Synthesized Sweeper and Agilent 8364A PNA. The output power of the intermodulation products at the upper and lower side bands was measured by an Agilent 8565E spectrum analyzer. Measurements were taken at 18 GHz, and a tone spacing of 4 MHz was chosen to avoid low-frequency dispersion. The source and load impedances were both set to 50 Ohm for all the measurements. Power gain  $G_p$  and  $IP_3$  were extracted from intermodulation distortion measurement and shown in Fig. 5 and Fig. 6.  $G_p$  and  $IP_3$  of Type-I/II DHBT increase monotonically with collector current density. While, for the two Type-I DHBTs,  $G_p$  increases with collector current density at first but fall off at high collector current density levels ( $J_c > 6 \text{ mA}/\mu\text{m}^2$ ).  $IP_3$  of the two Type-I DHBTs falls off at even lower collector current density level ( $J_c > 4 \text{ mA}/\mu\text{m}^2$ ). Comparing the  $f_T$  and  $IP_3$  curves, there is a correlation between  $IP_3$  and  $f_T$ . Less variant, monotonically increasing  $f_T$  will lead to higher  $IP_3$  (superior linearity) and  $f_T$  with more variance will lead to lower  $IP_3$  (inferior linearity). Thus, as an initial guess, we can estimate transistor nonlinearity from the  $f_T$  vs  $J_c$  curve. The  $f_T$  and  $IP_3$  fall off of Type-I DHBT at high current density is due to the base push out, current blocking and charge accumulation effects in the transition region.

#### CONCLUSIONS

A Novel Type-I/II submicron DHBT has been fabricated and characterized. Compared with Type-I DHBT, Type-I/II DHBT shows superior linearity performance due to its favorable band alignment.

#### REFERENCES

- [1] W. Snodgrass, W. Hafez, N. Harff, and M. Feng, Proceedings of the 2006 IEEE International Electron Devices Meeting (IEDM), San Francisco, CA, 11-13, December 2006, pp. 1-4.
- [2] K. Y. (Donald) Cheng, C.C. Liao, H. Xu, K.Y. Cheng, and M. Feng, Appl. Phys. Lett. **98**, 242103 (2011).
- [3] C. Nguyen, T. Liu, M. Chen, H. Sun, and D. Rensch, Proceedings of the IEEE International Electron Device Meeting (IEDM), Washington D.C., 10-13 December 1995, pp. 799-802.
- [4] K. Y. (Donald) Cheng, H. Xu, M. E. Stuenkel, E. W. Iverson, C. C. Liao, K. W. Yang, M. Feng, and K. Y. Cheng, J. Appl. Phys. **110**, 113703 (2011)
- [5] H. C. Poon, IEEE Transactions on Electron Devices, VOL. ED-21, No.1, January 1974.
- [6] M. Vaidyanathan, M. Iwamoto, L. E. Larson, P. S. Gudem, and P. M. Asbeck, IEEE Transactions on Microwave Theory and Techniques, vol. 51, no. 2, February 2003.

#### ACRONYMS

BCB: Bisbenzocyclobutene  
BJT: Bipolar Junction Transistor  
DHBT: Double Heterojunction Bipolar Transistor  
SHBT: Single Heterojunction Bipolar Transistor  
 $f_T$ : Current gain cutoff frequency  
 $f_{MAX}$ : Power gain cutoff frequency  
SOLT: Short-Open-Load-Through